

LCL-T Resonant Converter Based on Dual Active Bridge Topology in Solar Energy Applications

Alexander Vladimirovich Osipov¹, Yury Alexandrovich Shinyakov¹, Vadim Nikolaevich Shkolniy², Michael Sergeevich Sakharov¹

ABSTRACT: Resonant LCL-T converter can operate as stable voltage source, being fed from current, for instance, the photovoltaic battery. It is shown that LCL-T resonant tank has intrinsic ability to convert stable AC current into stable AC voltage thus parametrically regulating output voltage at a fixed value. This mode of operation is made possible by the use of active (synchronous) rectifier to recoup energy from the output back to the LCL-T resonant tank. Basic characteristics of resonant LCL-T converter regulated by phase shift between inverter and rectifier regardless of a solar battery current drift have been defined. It is shown that phase control guarantees 0 voltage and 0 current on switching; however, turn-off current could be substantial. Calculations and assumptions made in this study have been confirmed by simulation and hardware prototype.

KEYWORDS: Spacecraft power supply system, Resonant converter, Bidirectional dual active bridge, LCL resonant converter, ZVS, ZCS.

INTRODUCTION

Advancements in spacecraft (SC) power supply unit (PSU) are mostly related to enhancements in specific energy parameters, notably size, weight, and efficacy. Contemporary power converters in PSU are presented by non-isolated boost types controlled by pulse width modulation (PWM). The most prohibitive feature of such converters is hard commutation of switching devices, being a source of high losses as well as electromagnetic interference (EMI). The mitigation of hard switching shortcomings by introduction of various snubbing circuits to provide resonant switching transitions is not helpful due to added complexity and need for additional active elements to be commutated in the very same way (Pavlovic et al. 2012; Shiva Kumar et al. 2015; Bodur et al. 2003; Akin 2014; Goryashin and Khoroshko 2011). The commutation itself becomes too long and quite often creates unwanted oscillations thus increasing safety margin required and limiting conversion frequency as well as regulation range. All of this have led to the use of dual active bridge (DAB) resonant converters (Hillers et al. 2012; Selvaperumal et al. 2009; Sowjanya and Raghavendran 2013; Krismer and Kolar 2009; Osipov et al. 2015; Shivaraja 2015), including series LC tank, which is a resonant circuit. Sinusoidal waveform of inverter current automatically provides soft switching without auxiliary components. However, the energy source of SC PSU is usually a photovoltaic (PV) battery. It operates as current source while voltage is usually limited by isolation breakdown level in vacuum. At the same time load can vary a lot. Typical resonant LC converter cannot be used as a voltage regulator

¹Tomsk State University of Control Systems and Radioelectronics – Institute of Space Technologies – Research and Development Institute of Space Technologies – Tomsk/Tomsk – Russia. ²Reshetnev Company – Information Satellite Systems – Department 600 – Zheleznogorsk/Krasnoyarsk – Russia.

Author for correspondence: Alexander Vladimirovich Osipov | Tomsk State University of Control Systems and Radioelectronics – Institute of Space Technologies | 40 Lenina Prospect | 634050 – Tomsk/Tomsk – Russia | Email: ossan@mail.ru

Received: Jul. 26, 2016 | **Accepted:** Dec. 13, 2016

just because no-load condition will force the PV battery to operate in voltage source mode, creating high voltage across its terminals and increasing the possibility of breakdown.

The solution for this problem is the use of LCL-T converters (usually referred as “inductive-capacitive converter” in the Russian literature), typically applied as alternating current (AC) source and fed by stable AC voltage. The performance of such converters was analyzed in Russia (Milach *et al.* 1964; Dozorov 2013) and elsewhere (Borage *et al.* 2005; Borage and Tiwari 2012; Zouggar *et al.* 2000). However LCL converters can operate just in opposite way converting current source into voltage source, which is exactly the task the converter should perform in PV battery fed by PSU. In that case input current defines resonant tank 1, which, in turn, makes the value of AC voltage at resonant capacitor near constant regardless the load. Interestingly enough no investigations of such mode of operation could be referred to. To date published research papers describe the operation of LCL-T converter with diode-based (passive or uncontrollable) rectifier in output current stabilization mode, for instance, Borage *et al.* (2005). Therefore, the purpose of this study was to analyze resonant LCL-T converter in DAB configuration as voltage source mode being fed by PV battery operating in current source mode.

METHODOLOGY
LCL-T RESONANT CONVERTER OPERATION IN CURRENT-TO-VOLTAGE CONVERSION MODE

Transistors in resonant converters are commutated at the frequency near LC tank resonant 1, which provides sinusoidal current with near 0-value at switching instances, minimizing losses. Resonant tank can be loaded in different ways depending on the input source impedance. If the PV battery operates in voltage mode then the load is connected in series with the resonant tank (typical resonant DCDC converter) (Fig. 1a). If PV battery operates as current source the load is connected in parallel to the capacitor in resonant tank creating the so-called Boucherot circuit, in which circuit inverter’s output voltage is square by waveform. If the frequency equals to resonance 1 the current has sinusoidal waveform allowing switching transistors with minimal losses.

Regarding Boucherot circuit being fed by current source, capacitor’s current I_{Cn} amplitude is stable and actually does not depend on the load; correspondingly output voltage is stable, picked up at terminals of the capacitor C_n , and the value is defined by the equation

$$U_{out} = I_{PV} \cdot \rho \tag{1}$$

where: $\rho = \sqrt{L_n/C_n}$ is the tank’s characteristic impedance; L_n is the inductance value of resonant inductor L_n ; C_n is the capacitance value of resonant capacitor C_n .

Accordingly, varying parameters of the resonant tank 1 may match the current level of PV battery to the output voltage required without the use of transformer allowing to have output voltage lower than the input one, *i.e.* $R_L < \rho$, where R_L means load resistance.

In Buserot circuit (Fig. 1a) load current is the difference between capacitor and inverter ones, while capacitor’s current is stable by amplitude and is in phase with inverter’s voltage; inverter current is lagging voltage U_{inv} by angle α , depending on the load (Fig. 1b):

$$\alpha = \arctg \frac{\sqrt{L_n/C_n}}{R_L} = \arctg \frac{\rho}{R_L} \tag{2}$$

Voltage across the load U_{Cn} is shifted in respect to inverters one by $\pi/2$.

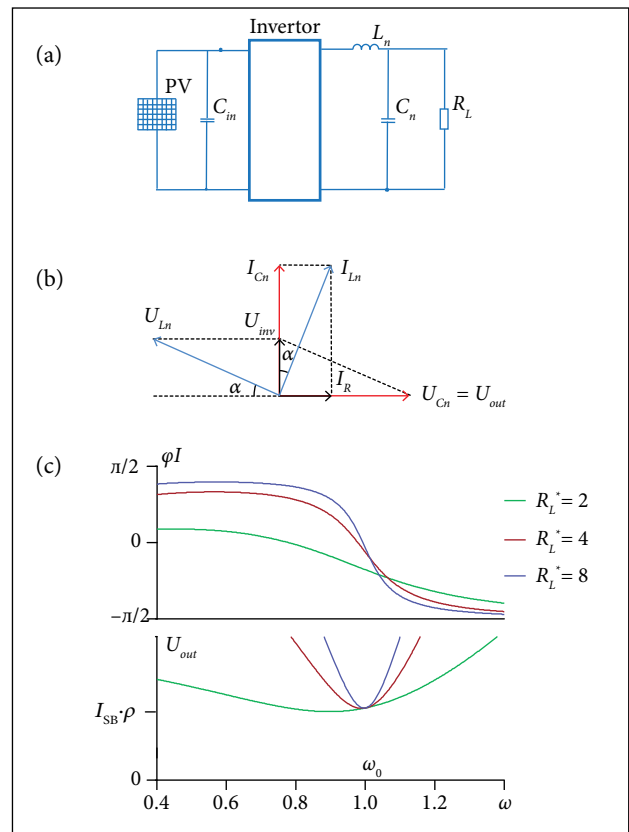


Figure 1. Series LC resonant converter. (a) Circuit; (b) Vector diagram; (c) Bode plot for phase and gain.

Frequency-related behavior of the resonant converter, plotted for different normalized load values $R_L^* = R_L/\rho$, is shown in Fig. 1c. It is clear that the shunting influence of the load shifts resonant frequency of the tank in accordance with

$$\omega_{res} = \sqrt{1/L_n C_n - 1/R_L^2 C_n^2} \tag{3}$$

If the frequency is fixed as $\omega_0 = \sqrt{1/L_n C_n}$ the load increase yields the phase shift defined in Eq. 2; in that case output voltage of an angular frequency ω_0 becomes stable due to compensation by the inductor current. Bode plot shows that load increase leads to the loss of converter resonance properties. To reduce phase shift due to the load change LCL-T topology may be used (Fig. 2).

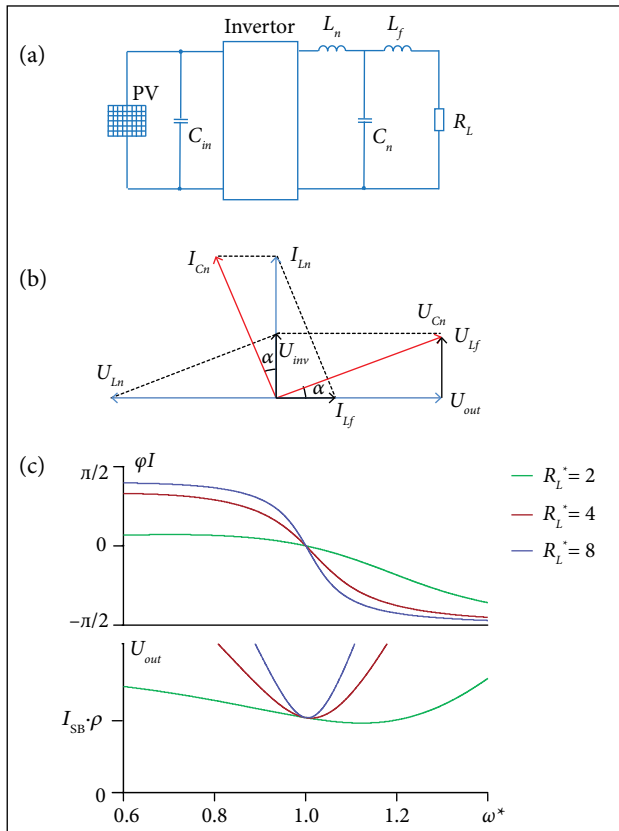


Figure 2. Resonant LCL-T converter. (a) Schematics; (b) Vector diagram; (c) Phase and amplitude responses.

The vector diagram of LCL-T converter (Fig. 2b) shows that in case of $L_n = L_f$ an additional voltage drop across L_f allows forming an angle equal to $\pi/2$ between the vectors of load current and inverter one regardless of the load. This condition can be met by the equality of right triangles formed

by the vectors U_{inv} , U_{L_n} , U_{C_n} , and U_R , U_{L_f} , U_{C_n} , which leads to $U_{L_n} = U_{out}$; the stability of output voltage because the change in U_{inv} is compensated by U_{L_f}

In that case the phase of capacitor current is shifted in regard to the inverter's one by the angle α defined by the load

$$\text{tg}\alpha = \frac{U_{PV}}{U_R} = \frac{I_L}{I_{inv}} = \frac{\rho}{R_L} \tag{4}$$

where: U_{PV} represents photovoltaic voltage.

Frequency-related parameters of LCL-T converter are shown in Fig. 2c. It can be observed that LCL-T tank allows stabilizing output voltage parametrically operating at the resonant frequency for the full load range.

LCL-T CONVERTER OPERATION ANALYSIS IN CURRENT-TO-VOLTAGE CONVERSION MODE WITH OUTPUT RECTIFIER

In order to supply constant output voltage one may need to use rectifier, bridge type, for instance (Fig. 3a), which substantially changes the converter behavior. Before anything else, the first harmonic experiences least resistance

$$R_{1M} = \frac{8}{\pi^2} R_L \tag{5}$$

as a result, the output voltage can be defined as

$$U_{out} = \frac{\pi^2}{8} I_{PV} \rho \tag{6}$$

So the resonant tank values could be defined as

$$C_n = \frac{I_{PV}}{U_{out}} \frac{\pi^2}{8} \frac{1}{\omega_0} \quad \text{and} \quad L_n = \frac{U_{out}}{I_{PV}} \frac{8}{\pi^2} \frac{1}{\omega_0} \tag{7}$$

The simulation for fixed output voltage $U_{out} = 100$ V, input current $I_{PV} = 8$ A, $f = 50$ kHz, and resonant tank parameters taken in accordance with Eq. 7 shows that output current is discontinuous, distorting rectifier input voltage U_{rect} , having $I_{L_f} = 0$ and $U_{rect} = U_{C_n}$ (Fig. 3b). The converter operates in non-resonant mode, and output voltage value does not comply with calculated value $U_{out} = 100$ V, increasing along with the load resistance. Idle operation is not possible. These problems can be partially solved by operating frequency adjustment (Boragay *et al.* 2005; Zouggar *et al.* 2000).

If one uses fully-controlled switches for rectifier, operation in continuous conduction mode could be forced and the aforementioned problems fixed by recouping energy from

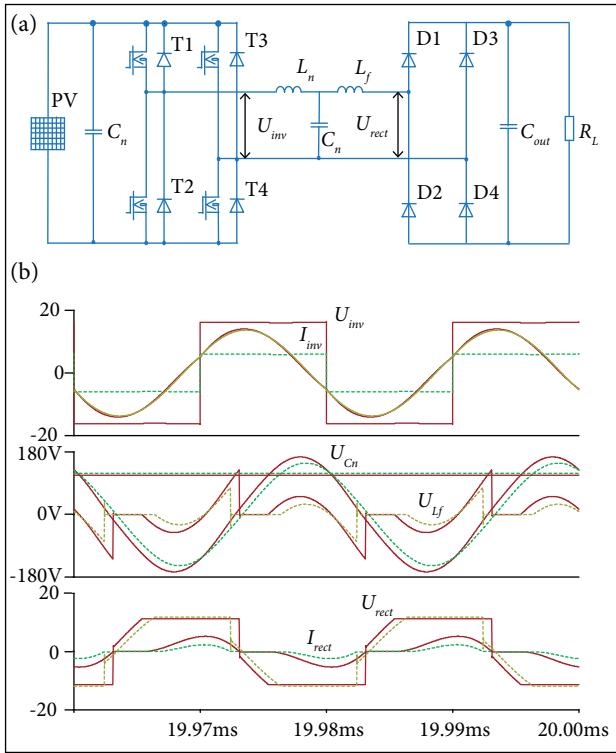


Figure 3. (a) Resonant LCL-T converter with non-active rectifier; (b) Operational waveforms at $U_{out} = 100$ V, $I_{pv} = 8$ A, and $f = 50$ kHz.

the output capacitor back to the resonant tank (Fig. 4a) thus making topology commonly referred as DAB. For proper operation output bridge control should be shifted by $\pi/2$ in respect to inverter. This is exactly the phase between inverter and load currents (Fig. 2b).

From the simulation it is clearly verified that, in order to stabilize output voltage at calculated value of $U_{out} = 100$ V, regardless of the load, one needs to operate at resonant point in continuous conduction mode for active rectifier I_{rect} (Fig. 4b). Rectifier current I_{rect} is not sinusoidal, being result of the application of 2 voltages to output inductor, rectangular U_{rect} , and sinusoidal U_{Cn} , which is specific to that topology. As a result rectifier current contains sinusoidal as well as saw tooth components:

$$I_{lf}(t) = I_{lf_saw}(t) + I_{lf_sin}(t) = \frac{U_{out}}{4L_f f} \cdot \frac{2t}{T} + \frac{4U_{out}}{\pi \omega L_f \cos \alpha} \cdot \cos(\omega t + \alpha) \quad (8)$$

Rectifier current diagrams for a different load values are

shown in Fig. 5. For instance, at no load or idle capacitor's, voltage is in phase with rectifier's voltage, $\alpha = 0$; saw tooth

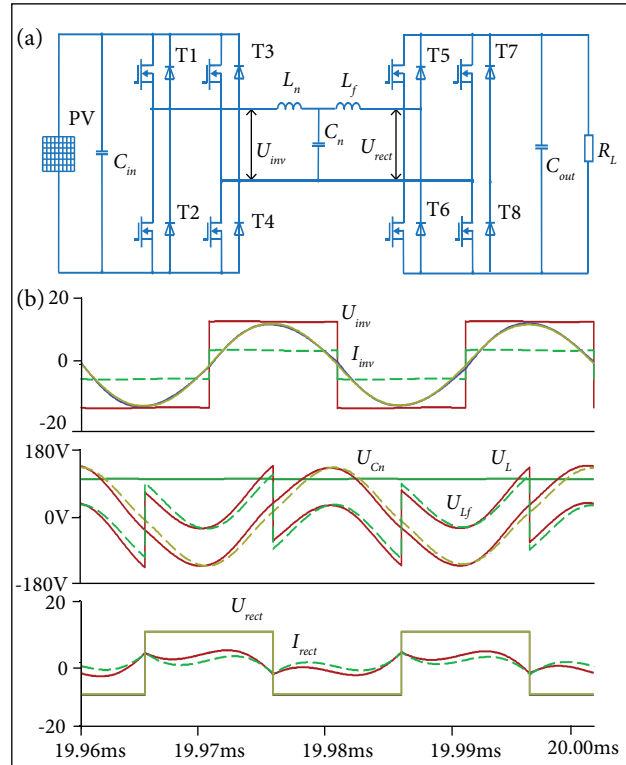


Figure 4. (a) Resonant LCL converter in DAB configuration schematics; (b) Operational waveforms at $U_{out} = 100$ V, $I_{pv} = 8$ A, and $f = 50$ kHz.

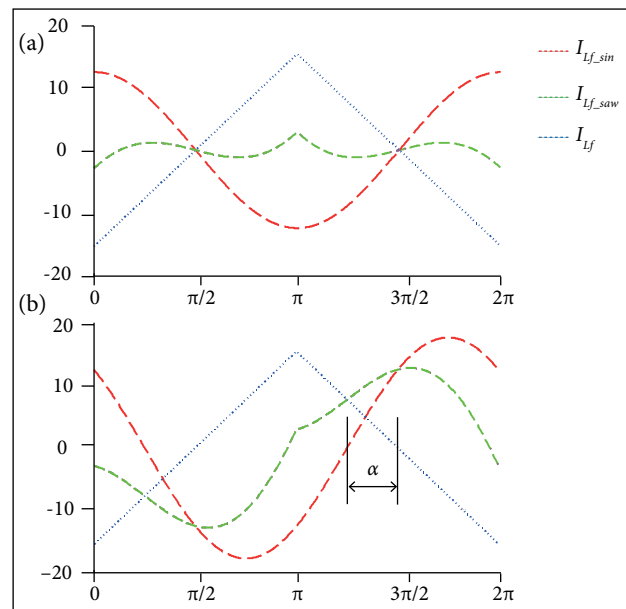


Figure 5. Rectifier input current at the idle. (a) At normalized load (no-load operation); (b) Nominal load operation: $R_L = \pi 2/8p$.

as well as sinusoidal components in current do have equal fundamental harmonic and, correspondingly, there is no fundamental harmonic in the output current. Besides, averaged rectified current is equal to 0 (Fig. 5a).

As we increase the load phase shift between capacitor and rectifier voltages, α starts to appear, and capacitor's voltage starts (Fig. 5b). In the case when $R_H = \pi^2/8\rho$, i.e., at the value $R_H^* = 1$, phase shift $\alpha = \pi/4$ and rectifier's current contains fundamental harmonic

$$I_{rect_1m} = \frac{\pi}{2} I_{PV} \tag{9}$$

This way output current depends on load phase angle α .

PHASE SHIFT CONTROL OF LCL-T RESONANT CONVERTER

One of the most important PV battery features is instability of the output current level, which depends on quite a few external conditions like illumination change during shade-light transition, efficiency degradation due to radiation, etc. Such effects can be compensated by the shifting control of rectifier U_{rect} in respect to inverter voltage U_{inv} by phase β . For classic DAB implementation, such method of control is described in Pavlovic *et al.* (2012). As a result of current recoup into a resonant tank, output voltage would rise. The process of control is shown in details in the vector diagram of Fig. 6a.

If we shift rectifier control by the angle β it shifts rectifier current phase to the very same value in respect to rectifier input voltage, forcing output voltage U_{out} to rise in accordance with

$$U_{out} = \frac{\pi^2}{8} I_{PV} \rho \cdot \frac{1}{\cos \beta} \tag{10}$$

It is very important to hold phase shift of $\pi/2$ between inverter voltage U_{inv} and rectifier current I_{rect} to provide conditions for parametric stabilization of the output voltage, because it will preserve the equality of triangles formed by the vectors U_{inv} , U_{Ln} , U_{Cn} and U_{rect} , U_{Lf} , U_{Cn} , respectively.

Angle α is determined by the load value similarly to the previous case and could be calculated as follows:

$$\alpha = \beta - \arctg \left(\tg \beta - \frac{1}{R_L^* \cos^2 \beta} \right) \tag{11}$$

where: $R_L^* = (8/\pi^2)(RL/\rho)$ is the normalized load value.

Angle α , in turn, defines voltage across C_n :

$$U_{Cn} = \frac{\pi}{2} \cdot \frac{1}{\cos(\beta - \alpha)} I_{PV} \rho \quad \text{and} \tag{12}$$

$$U_{Cn}^* = \frac{\pi}{2} \cdot \frac{1}{\cos(\beta - \alpha)}$$

Regulation curves are shown in Fig. 7. It is clear that the angle of control α depends on the control angle β , while minimum capacitor voltage occurs if $\alpha = \beta$, and it corresponds to $U_{Cn}^* = (\pi/2)(1/\cos\beta)$; in case of $\beta = \pi/4$ and $R_L^* \rightarrow \infty$, the voltage across C_n would be $U_{Cn}^* = (\pi/\sqrt{2})$.

For a given case there are diagrams shown in Fig. 6b. If PV battery current is decreased to $I_{PV} = 5.6$ A, $\sigma I_{PV} = \sqrt{2}$ and $R_L^* = 2$, in accordance with Eq. 10; to produce previous output voltage level, control angle $\beta = \pi/4$ is necessary, meaning $\alpha = \beta$. Thus using Eq. 12 we can derive $U_{Cn} = (2\sqrt{2}/\pi)U_{out}$, which is shown in the diagram of Fig. 6b.

Commutation mode of switches in LCL-T converter using phase regulation: the condition necessary for ZVS is the lag of rectifier voltage in respect to inverter's voltage by $\pi/2 + \beta$.

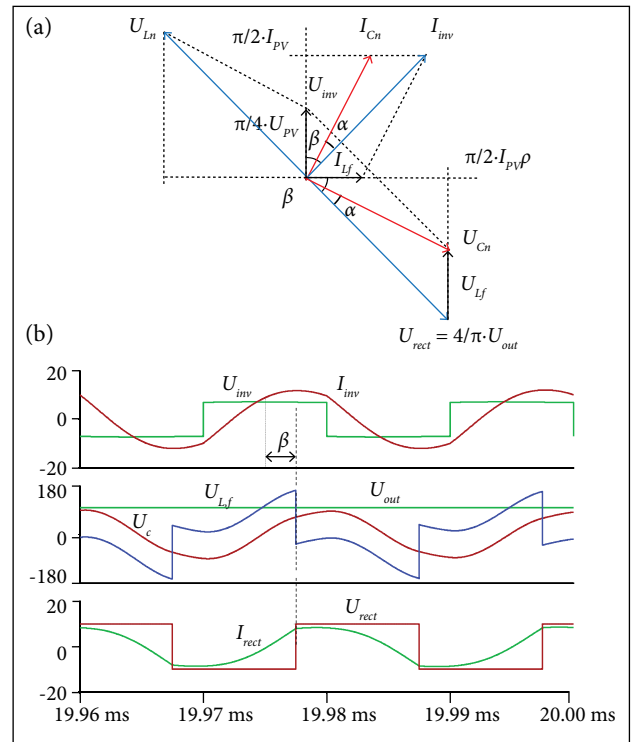


Figure 6. Phase regulation in resonant LCL-T converter with active rectifier: (a) LCL-T converter vector diagram of phase regulation process; (b) Operation diagram at $I_{PV} = 5.6$ A, $\beta = \pi/4$, $R_L = 25 \omega$, and $R_L^* = 2$.

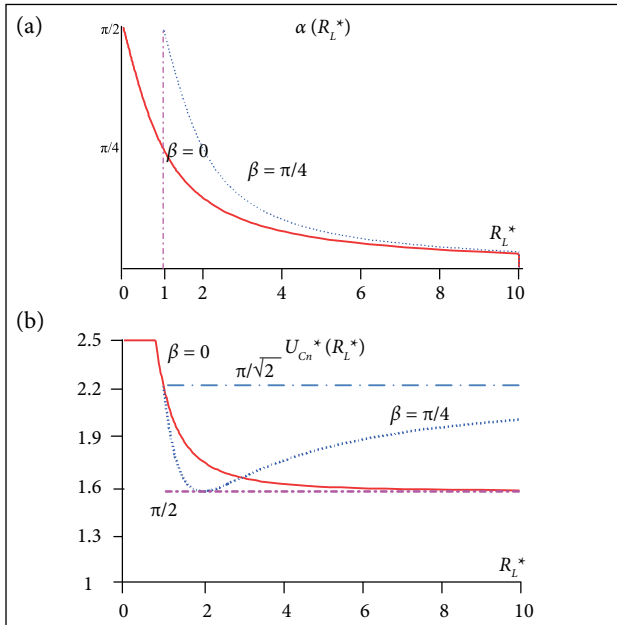


Figure 7. (a) Control angle α ; (b) Resonant capacitor voltage, U_{Cr} , versus normalized load in the LCL converter.

Such control mode provides conditions for turning transistors ON. Commutation transitions depend on a bridge place. In the inverter, one has to make commutation before the current changes the sign (Fig. 8b), which provides turning in the complementary switch at reverse bias or 0 voltage across. In rectifier, one has to make commutation after the change of the current sign (Fig. 8). This way, in order to provide ZVS, one has to supply a leading current phase of the inverter and a lagging one for the rectifier.

Turn off transition occurs at rather high current; however, proper snubbing capacitor across the switch or even transistor's output capacitance together with dead time adjustment does provide proper commutation.

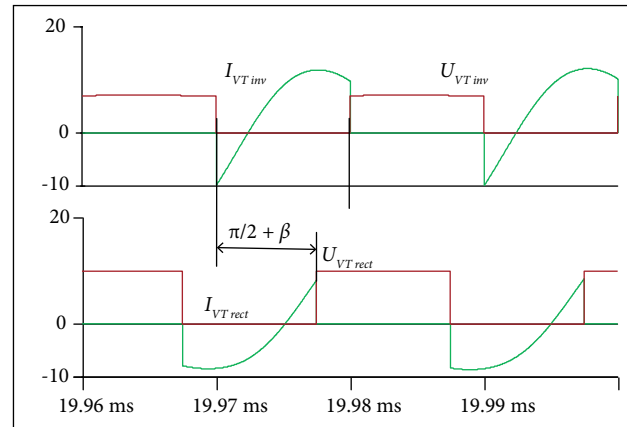


Figure 8. Current and voltage waveforms of rectifier and inverter in resonant LCL-T converter using phase control.

RESULTS

The components used in hardware prototype are shown in Table 1. To verify simulation data hardware prototype has been built (Fig. 4a) Actual operation diagrams are presented in Fig. 9. The parametric stabilization obtained 2%, and soft commutation could be observed in all cases.

It is shown that, if input current amplitude is held constant at 0.86 A (using hardware PV battery simulator IPV-200/7-4),

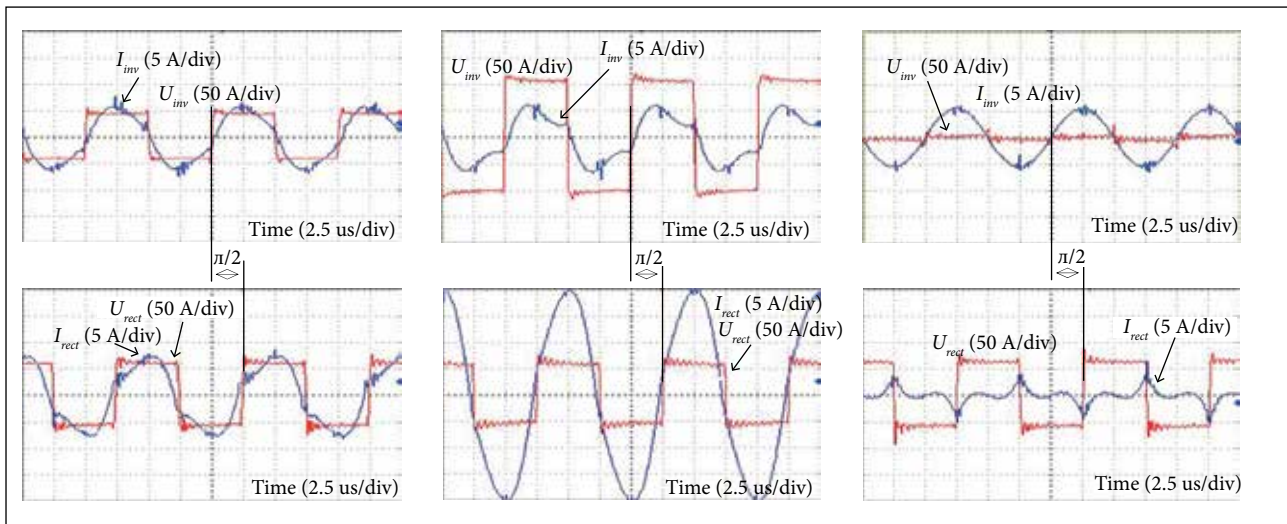


Figure 9. Operating diagrams for different load values of the LCL-T converter. (a) $R_L = 18 \Omega$; (b) $R_L = 6 \Omega$; (c) Idle ($R_L = \infty$).

then output voltage stays at 60 V. Variation of the load resistance does change input current consumed.

Table 1. Components used in the hardware prototype.

| Part | Value |
|---------------------------|--------------------------|
| T1... T8 | IRFP4668 |
| $L_n = L_f$ | 15.6 μH^* |
| C_n | 0.165 μF^{**} |
| Conversion frequency | 102 kHz |
| Primary power source type | IPV-200/7-4 |
| Input current I_{PV} | 3.2 A |
| Load resistance | 6... $\infty \Omega$ |

*ETD34/17/11 N = 28 turns; **K78-2-315B-0.033 μF 5 pcs.

CONCLUSION

Resonant LCL-T converter has the ability to convert the current source into the voltage one, which best serves for SC PSU where the primary source is PV battery. Through the use of an active rectifier, LCL-T converter provides high accuracy of parametric stabilization of the output voltage from the idle

up to the full load. Moreover, for operation at the idle unlike the state-of-the-art prototypes (Pavlovic *et al.* 2012; Hillers *et al.* 2012; Selvaperumal *et al.* 2009), there is no need for frequency adjustment, which in turn eases control effort.

ACKNOWLEDGMENTS

The study was performed during the execution of a complex project (number 02.G25.31.0182) with the financial support of the Russian Government (Ministry of Education of Russia).

AUTHOR'S CONTRIBUTION

Osipov AV, Shinyakov YA, and Shkolniy VN conceived the idea and co-wrote the main text; Osipov AV and Sakharov MS performed the experiments; Sakharov MS prepared the figures. All authors discussed the results and commented on the manuscript.

REFERENCES

- Akin B (2014) An improved ZVT-ZCT PWM DC-DC boost converter with increased efficiency. *IEEE Trans Power Electron* 29(4):1919-1926. doi: 10.1109/TPEL.2013.2269172
- Bodur H, Bakan AF, Baysal M (2003) A detailed analytical analysis of a passive resonant snubber cell perfectly constructed for a pulse width modulated d.c.-d.c. buck converter. *Electr Eng* 85(1):45-52. doi: 10.1007/s00202-002-0141-7
- Borage M, Tiwari S (2012) AC analysis of resonant converters using PSpice. A quicker approach. *Asian Power Electronics Journal* 6(2):1-6.
- Borage M, Tiwari S, Kotaiah S (2005) Analysis and design of an LCL-T resonant converter as a constant-current power supply. *IEEE Trans Ind Electron* 52(6):1547-1554. doi: 10.1109/TIE.2005.858729
- Dozorov SA (2013) Research and development of inductive-capacitive power source (PhD thesis). Saint Petersburg: Saint Petersburg Electrotechnical University "LETI". In Russian.
- Goryashin NN, Khoroshko AY (2011) On increasing the energy efficiency of a pulsed voltage converter with a resonant switching. *Bulletin SibSAU* 4(37):20-24.
- Hillers A, Christen D, Biela J (2012) Design of a highly efficient bidirectional isolated LLC resonant converter. *Proceedings of the 15th International Power Electronics and Motion Control Conference*.
- Krismser F, Kolar JW (2009) Accurate small-signal model for the digital control of an automotive bidirectional dual active bridge. *IEEE Trans Power Electron* 24(12):2756-2768. doi: 10.1109/TPEL.2009.2027904
- Milach AN, Kubyskin BE, Volkov IV (1964) Inductive-capacitive voltage

converters in current sources. Kiev: Naukova Dumka.

Osipov AV, Shinyakov Yu A, Chernaya MM, Tkachenko AA (2015) Resonant converters Solar energy. *Proceedings of the 19th International Scientific Conference "Reshetnev's Readings"*. Krasnoyarsk; Russia.

Pavlovic Z, Oliver J, Alou P, Garcia O, Cobos J (2012) Bidirectional dual active bridge series resonant converter with pulse modulation [accessed 2016 Jun 3]. https://www.researchgate.net/publication/254019572_Bidirectional_Dual_Active_Bridge_Series_Resonant_Converter_with_pulse_modulation

Selvaperumal S, Christober C, Rajan A (2009) Embedded control of LCL resonant converter analysis, design, simulation and experimental results. *Engineering* 1(1):7-15. doi: 10.4236/eng.2009.11002

Shiva Kumar S, Panda AK, Ramesh T (2015) A ZVT-ZCT PWM synchronous buck converter with a simple passive auxiliary circuit for reduction of losses and efficiency enhancement. *Ain Shams Engineering Journal* 6(2):491-500. doi: 10.1016/j.asej.2014.10.018

Shivaraja L (2015) Modeling and simulation of LLC resonant converter for photovoltaic systems. *International Journal of Emerging Technology and Innovative Engineering* 1(4):175-179.

Sowjanya K, Raghavendran P (2013) Isolated bidirectional full-bridge DC-DC converter with a flyback snubber. *International Journal of Soft Computing and Engineering* 3(2):16-25.

Zouggar SH, Charif N, Azizi M (2000) Neural control and transient analysis of the LCL-type resonant converter. *Eur Phys J Appl Phys* 11(1):21-27. doi: 10.1051/epjap:2000142